

Suprathermal Electron Generation and Channel Formation by an Ultrarelativistic Laser Pulse in an Underdense Preformed Plasma

G. Malka,¹ J. Fuchs,^{2,3} F. Amiranoff,³ S. D. Baton,³ R. Gaillard,^{1,*} J. L. Miquel,¹ H. Pépin,²

C. Rousseaux,¹ G. Bonnaud,¹ M. Busquet,¹ and L. Lours¹

¹Commissariat à l'Énergie Atomique, Limeil-Valenton, 94195 Villeueuve-Saint-Georges Cedex, France

²INRS-Énergie et Matériaux, 1650 bd. L. Boulet, J3X1S2 Varennes, Québec, Canada

³Laboratoire pour l'Utilisation des Lasers Intenses, CNRS, École Polytechnique, 91128 Palaiseau Cedex, France

(Received 29 January 1997)

Relativistic electrons are produced, with energies up to 20 MeV, by the interaction of a high-intensity subpicosecond laser pulse ($1 \mu\text{m}$, 300 fs, 10^{19} W/cm^2) with an underdense plasma. Two suprathermal electron populations appear with temperatures of 1 and 3 MeV. In the same conditions, the laser beam transmission is increased up to 20%–30%. We observe both features along with the evidence of laser pulse channeling. A fluid model predicts a strong self-focusing of the pulse. Acceleration in the enhanced laser field seems the most likely mechanism leading to the second electron population. [S0031-9007(97)03893-3]

PACS numbers: 52.40.Nk, 52.25.Rv, 52.50.Jm, 52.70.Kz

With the progress of compact short-pulse multiterawatt laser systems [1], it has become possible to produce MeV electrons in a plasma as seen in recent experiments with solid targets [2], preformed plasmas [3], or pulsed gas jets [4]. The fast ignitor concept [5], relevant to the inertial confinement fusion (ICF), enhances the interest in this process as well as in laser propagation and channel formation. In an underdense plasma, electrons and ions tend to be expelled from the focal spot by the ponderomotive pressure of an intense laser pulse, and the channel [6,7] can act as a propagation guide for the laser beam. Depending on the quality of the laser beam, the cumulative effects of ponderomotive and relativistic self-focusing [8] can significantly increase the laser intensity. For these laser pulses, the laser electric and magnetic fields reach few hundreds of GV/m and megagauss, respectively, and the electron quiver velocity in the laser field is closed to the light speed. The component of the resulting Lorentz force ($-e\mathbf{v} \times \mathbf{B}$) accelerates electrons in the longitudinal direction, and energies of several tens of MeV can be achieved [9]. 3D particle-in-cell (PIC) simulations have also shown these features [10]. Besides the direct electron acceleration by the laser fields, the forward Raman scattering instability (FRS) can also accelerate electrons to MeV energies in the underdense plasma [4]. The efficiency of the latter process strongly depends on the laser intensity [11–13] and on the density profile of the surrounding medium (hollow channel or weakly perturbed plasma) [12,14,15]. It is thus directly related to the ability of the short pulse to be transmitted.

In this Letter, we present direct measurements of MeV electrons produced by the interaction of an intense subpicosecond laser pulse with an underdense plasma in the relativistic regime ($n/n_c \approx 0.1$ – 0.2 , where n is the electron density and n_c is the critical density, $n_c \approx 10^{21} \text{ cm}^{-3}$ for a $1 \mu\text{m}$ laser wavelength). We also present shadowgraphs showing channel formation, and laser pulse transmission

measurements that show an increase of the transmission with the pulse intensity.

The experiments are performed with the P102 laser system [1] at CEA/LV. A creation laser beam is focused by a $f/6$ lens through a random phase plate onto a thin plastic foil (CH 3000 Å), 35° above the target normal (see Fig. 1). The $1.058 \mu\text{m}$ –750 ps FWHM laser pulse has an average intensity of $(3\text{--}5) \times 10^{12} \text{ W/cm}^2$ (90% of 5 J contained in a $400 \mu\text{m}$ focal spot). After a time delay, the subpicosecond laser interaction beam is focused with a $f/3$ off-axis parabola at normal incidence onto the rear side of the heated target. This $1.058 \mu\text{m}$ 300–500 fs FWHM interaction beam has an energy up to 15 J, an elliptical focal spot of $5 \times 10 \mu\text{m}^2$ containing 20% of the laser energy. This leads to a peak intensity of 10^{19} W/cm^2 . The rest of the energy is spread over a large area and does not contribute to the high-intensity interaction. The intensity contrast ratio between the short pulse and the background light, including the prepulses, is $10^8:1$ up to about 50 ps before the maximum. A probe beam ($0.53 \mu\text{m}$, 1 ps) is fired 10 to 20 ps after the interaction beam. It is used for transverse shadowgraphy of the plasma. The energy of the intense beam which is transmitted through the plasma is collected by a $f/1.3$ optics and focused on a fast photodiode (100 ps rise

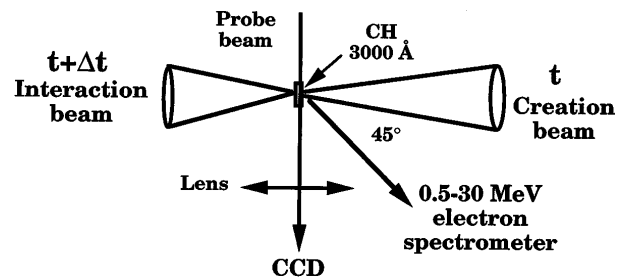


FIG. 1. Top view of the experimental setup.

time). High-energy electrons in the range 0.5–30 MeV are measured by a mirror spectrometer [16] and eight thick silicon diodes at 45° from the laser propagation axis and with an acceptance solid angle of 5×10^{-4} sr. The electron density profiles are calculated from the creation laser pulse using the 1D hydrocode (CHIVAS) [17]. By the time the interaction takes place (500–850 ps after the maximum of the creation pulse), the plasma is fully ionized, the maximum density is approximately equal to $0.2n_c$ and $0.1n_c$, respectively, and the plasma is several hundred microns long. These estimates compare favorably with the shadowgraphs at different delays.

The channeling, produced by the interaction laser pulse, is observed on the probe beam shadowgraphs. For the shot in Fig. 2, the time delay after the creation beam is 500 ps, corresponding to a maximum electron density about $0.2n_c$. Clear diffraction fringes are seen parallel to the interaction beam path. This is probably caused by a strong optical index perturbation due to the plasma depletion under the action of the interaction beam. It is not due to a density increase on axis since the plasma is already fully ionized. The channel is approximately 40 μm wide, a few times the laser focal diameter. This expansion is due to a supersonic radial shock wave propagating between the interaction beam and the probe beam [7].

Since, at these high intensities, the density depletion occurs during the interaction, we expect ponderomotive self-focusing [8] to occur. It could be further enhanced by relativistic self-focusing. Indeed, the laser power is far above the critical power (≈ 1 TW) [8]. Of course, as self-focusing occurs through the plasma, the beam intensity increases and strengthens the density depletion as the pulse moves inward.

To look at the variation of self-focusing with laser intensity and plasma density, we developed a code using

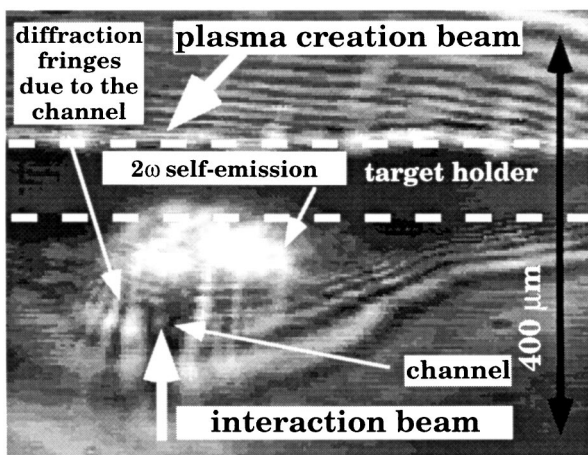


FIG. 2. Transverse shadowgraph of the plasma 500 ps, after the creation beam, showing the channeling in the underdense plasma. Creation beam energy: 4.5 J; interaction beam energy: 8 J ($I_{\text{max}} \approx 6 \times 10^{18}$ W/cm 2), CH 3000 Å. The delay between the probe beam and the interaction beam is 10–20 ps.

standard paraxial wave propagation in cylindrical geometry (for details see [18]). The code simulates the propagation of a high-intensity laser pulse in a flat underdense plasma [beginning by a $\tanh(z)$ ramp]. This code includes diffraction and relativistic change of the electron mass. In addition, we take into account the self-consistent density perturbation due to the laser pulse. In the hydrodynamic model used for this purpose, both ions and electrons are mobile, and full nonlinearity of the fluid equations is taken into account. The thermal pressure is neglected since, at those intensities, the ponderomotive pressure near the laser axis is far above the kinetic pressure. The evolution of the peak pulse intensity along the propagation axis is presented in Fig. 3 for the same parameters as in Fig. 2 ($n/n_c = 0.2$ and $I = 6 \times 10^{18}$ W/cm 2 at the vacuum waist position). The calculation shows the self-focusing of the laser pulse which increases the laser intensity up to a few times 10^{20} W/cm 2 , two hundred microns before reaching the focal position in vacuum. In this code, the plasma density reaches fast and complete cavitation as soon as the pulse intensity exceeds a few times 10^{19} W/cm 2 . We emphasize that, in order to obtain intensity levels about 10^{20} W/cm 2 , both the initial laser intensity and plasma density have to be sufficiently high (about 2×10^{18} W/cm 2 at the edge of the interaction zone and 10^{20} W/cm $^{-3}$, respectively). Using these results, the features in Fig. 2 can be better understood. The diffraction fringes become stronger along the path since plasma depletion increases along the laser propagation. The strong second harmonic self-emission due to the interaction beam is also understood to appear at that location (near the end of the channel) since it is maximized where radial index gradients are maximum.

The transmission of the interaction beam through the entire length of the preformed plasma is shown in Fig. 4 for a 850 ps delay ($n_{\text{max}} \approx 0.1n_c$). Up to an interaction beam intensity of 4×10^{18} W/cm 2 , where only one electron temperature is observed [see Fig. 5(b) discussed below] and where the simulated self-focusing process appears weak, the transmission stays about 5%. At higher

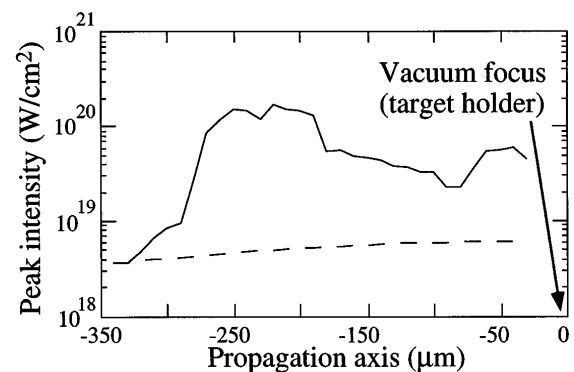


FIG. 3. Simulation of Gaussian interaction beam intensity along the propagation axis. Dashed line: vacuum propagation (the waist position is at 0); solid line: underdense plasma propagation. Same parameters as in Fig. 2.

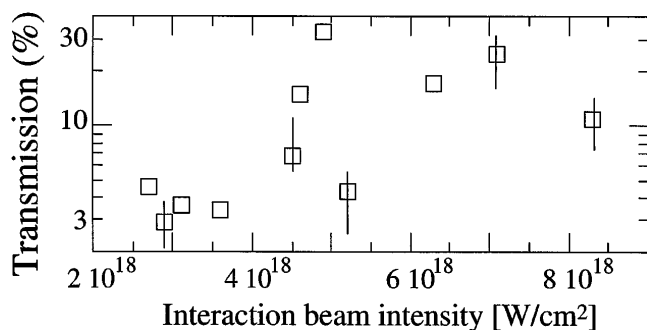


FIG. 4. Interaction beam transmission in the underdense plasma versus intensity. The strong increase in transmission is correlated with the appearance of a second hot electron temperature and the consistent calculation of self-focusing. Experimental conditions are creation beam energy about 5 J ($I_{\max} \approx 3.5 \times 10^{12}$ W/cm²), 3000 Å CH target. The delay between the interaction beam and the creation beam is 850 ps (peak density about $0.1n_c$).

intensities ($\geq 5 \times 10^{18}$ W/cm²), in the conditions where two electron temperatures are observed and where the simulations show both a strong self-focusing up to a few times 10^{20} W/cm² and the formation of a hollow channel, transmission increases up to 20%–30%. Such behavior could be related to channel formation and a weakening of Raman scattering, as discussed below.

The electron energy distribution obtained for the same laser shot as in Fig. 2 is plotted in Fig. 5(a). For electrons with energies between 0.5 and 5 MeV, the temperature is equal to about 1 MeV. Electrons with energies higher than 5 MeV are characterized by a warmer temperature of 3 MeV. The maximum observed energy is 20 MeV. In the same plasma conditions, we observe a threshold for the observation of the second temperature: Up to 4×10^{18} W/cm² (where the transmission is low), only one temperature is observed as shown in Fig. 5(b). It is very interesting to note that 3D PIC simulations [10] with similar laser and plasma parameters (10^{19} W/cm², 1 μ m, $n/n_c = 0.36$) show relativistic self-focusing, channel formation, and plasma cavitation, leading (i) to the increase of the on-axis laser intensity up to 2×10^{20} W/cm² and (ii) to accelerated electrons with a hot temperature between 3 and 5 MeV. The two possible explanations for these high-energy electrons are either a direct acceleration via the Lorentz force of the enhanced laser intensity in the channel [10,19] or an acceleration in the plasma waves generated by FRS in the channel.

The maximum energy gain of an electron accelerated in the plasma wave generated by FRS depends on its phase velocity, e.g., on the density [20]. The maximum energy of an initially slow electron doing a single trip in the plasma wave is $E_{\max} = mc^2 \gamma_\phi \gamma (1 + \beta_\phi \beta)$, where γ_ϕ is the relativistic factor of the wave propagating at the phase velocity $c\beta_\phi$ [$\gamma_\phi = 1/(1 - \beta_\phi^2)^{1/2}$]. The maximum energy of the electron in the wave frame γ is given

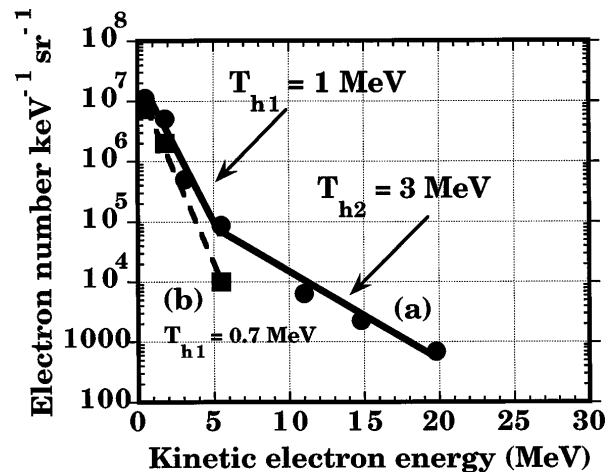


FIG. 5. Electron populations: (a) Circles = data and solid line = fit. The two beams are used with a delay $\Delta t = 500$ ps. The interaction beam intensity is $I_{\max} \approx 6 \times 10^{18}$ W/cm² (same shot as in Fig. 1). $T_{h1} \approx 1$ MeV and $T_{h2} \approx 3$ MeV. (b) Squares = data and dashed line = fit. Same underdense plasma conditions but $I \approx 3 \times 10^{18}$ W/cm² and $T_h \approx 0.7$ MeV. The data are fitted with single or double Maxwellian distributions.

by $\gamma = 1 + 2\gamma_\phi \beta_\phi^2 \alpha$, where $\alpha = \delta n/n_e$ is the normalized amplitude of the electron density perturbation ($\alpha \sim 1$ at wave breaking). In the case of FRS, we obtain $\beta_\phi = \sqrt{x}/(\sqrt{1-x} - \sqrt{1-2\sqrt{x}})$, where $x = n_e/n_c$. To obtain a maximum energy of 20 MeV (as observed for the second hot temperature) the density has to be lower than $n/n_c \sim 0.07$. In the channel, all plasma densities are explored, making it possible for the FRS instability to play a significant role. However, for intensities exceeding 10^{18} W/cm² (near our transmission threshold), the FRS relativistic growth rate is shown to decrease [11,12]. Moreover, in a depressed channel, FRS is either eliminated or greatly reduced [11,14] due to the nonresonant coupling between the laser field and the surface modes, as already observed in [15] at similar laser intensities. This concept is in good agreement with our observations and self-focusing simulations: High intensity and channel formation (i) guide the laser pulse and (ii) reduce the FRS, leading to a better transmission than at lower intensities. We believe that these observations are indeed characteristic of our high-density/high-intensity channeled propagation regime, and differ somewhat from the low-density/low-intensity regime observed elsewhere [21]. Furthermore, 2D PIC simulations at ultrahigh intensities [19] show strongly heated electrons, even in the absence of significant FRS.

In the case of direct electron acceleration by an intense laser field ($I \approx 10^{20}$ W/cm²) in vacuum [9], the emission angle of the electrons is reduced as the energy gain increases. For an electron initially at rest and accelerated up to 20 MeV, the half-angle of the emission cone is limited to 12° , whereas we observe these electrons at

45°. However, electrons with an initial kinetic energy can cross the accelerating laser field at an angle and be ejected this way. Furthermore, electrostatic interactions or strong toroidal self-generated magnetic fields [10] due to the accelerated on-axis electrons [7] can curve the electron trajectories and modify the ejection angles.

For the electrons with energies up to 5 MeV (first hot temperature) accelerated by plasma wave breaking, and using the previous formula for E_{\max} , we see that n/n_c has to be lower than 0.18. This corresponds to our plasma conditions at the time when the interaction takes place. For large delays (>800 ps), i.e., when $n/n_c < 10\%$ and when the plasma is longer, the warmer population disappears. This is in agreement with our calculations which show that the self-focusing process is less efficient at low plasma densities.

In summary, we observe in the interaction of a relativistic short laser pulse with a preformed underdense plasma, for the first time, two hot electron populations and enhanced transmission. These observations are successfully modeled by simulations of channeling and self-focusing of the laser pulse. Similar features have already been simulated using a 3D PIC code in the same conditions as ours [10]. Since the short pulse transmission increases with the intensity, the FRS instability may not play a significant role in the formed channel. Therefore, the increasing laser field seems to be the most likely mechanism to lead to such electron acceleration. These results are of great interest in the context of the fast ignitor concept since (i) the formation of a channel facilitates the laser pulse propagation through the corona of the ICF targets, (ii) the high transmission rate means propagation without significant energy loss, and (iii) MeV electrons are required to produce the hot spot in the compressed fuel.

We would like to thank T. Johnston, D. Juraszek, E. Lefebvre, J. Meyer-ter-Vehn, A. Modena, and P. Renaudin for fruitful discussions, and R. Wrobel for lending the electron spectrometer. We also wish to acknowledge

encouragement and support from A. Jolas, as well as N. Blanchot, the technical assistance of the P102-Castor staff at CEA Limeil, and R. Caland for target fabrication.

*Present address: Imperial College, The Blackett Laboratory, Prince Consort Road, London SW7-2AZ, England.

- [1] N. Blanchot *et al.*, *Opt. Lett.* **20**, 395 (1995).
- [2] G. Malka and J.L. Miquel, *Phys. Rev. Lett.* **77**, 75 (1996).
- [3] C. Darrow *et al.*, *SPIE* **1860**, 46 (1993).
- [4] A. Modena *et al.*, *Nature (London)* **377**, 6 (1995).
- [5] M. Tabak *et al.*, *Phys. Plasmas* **1**, 1626 (1994).
- [6] A. Borisov *et al.*, *Phys. Rev. A* **45**, 5830 (1992); P. Monot *et al.*, *Phys. Rev. Lett.* **74**, 2953 (1995); P. Young *et al.*, *Phys. Rev. Lett.* **75**, 1082 (1995); A. Chiron *et al.*, *Phys. Plasmas* **3**, 1373 (1996); M. Borghesi *et al.*, *Phys. Rev. Lett.* **78**, 879 (1997).
- [7] J. Fuchs *et al.*, *Phys. Rev. Lett.* (to be published).
- [8] G. Mainfray and C. Manus, in *Progress in Optics*, edited by E. Wolf (North-Holland, Amsterdam, 1993), Vol. 32, p. 313; A. Borisov *et al.*, *Plasma Phys. Controlled Fusion* **37**, 569 (1995).
- [9] F.V. Hartemann *et al.*, *Phys. Rev. E* **51**, 4833 (1995); G. Malka, E. Lefebvre, and J.L. Miquel, *Phys. Rev. Lett.* **78**, 3314 (1997).
- [10] A. Pukhov and J. Meyer-ter-Vehn, *Phys. Rev. Lett.* **76**, 3975 (1996).
- [11] C.D. Decker *et al.*, *Phys. Rev. E* **50**, R3338 (1994).
- [12] W.B. Mori *et al.*, *Phys. Rev. Lett.* **72**, 1482 (1994).
- [13] K.C. Tzeng *et al.*, *Phys. Rev. Lett.* **76**, 3332 (1996).
- [14] T.C. Chiou *et al.*, *Phys. Plasmas* **3**, 1700 (1996); C.S. Liu and V.K. Tripathi, *Phys. Plasmas* **3**, 3410 (1996).
- [15] A. McPherson *et al.*, *J. Phys. B* **29**, L291 (1996).
- [16] S. Fontenay, Ph.D. thesis, Paris-Sud University, 1995 (unpublished).
- [17] S. Jacquemot and A. Decoster, *Laser Part. Beams* **9**, 517 (1991).
- [18] V. Biancalana and P. Chessa, *Appl. Opt.* **33**, 3465 (1994).
- [19] D. Forslund *et al.*, *Phys. Rev. Lett.* **54**, 558 (1985).
- [20] P. Mora and F. Amiranoff, *J. Appl. Phys.* **66**, 3476 (1989).
- [21] C. Coverdale *et al.*, *Phys. Rev. Lett.* **74**, 4659 (1995).